

# Chemical Interaction Between Fe and Silicon Nitride Ceramic

E. Heikinheimo,<sup>a</sup> I. Isomäki,<sup>a</sup> A. A. Kodentsov<sup>b</sup> & F. J. J. van Loo<sup>b,\*</sup>

<sup>a</sup>Helsinki University of Technology, Laboratory of Metallurgy, FIN-02150 Espoo, Finland

<sup>b</sup>Eindhoven University of Technology, Laboratory of Solid State Chemistry & Materials Science, NL-5600 MB Eindhoven, The Netherlands

(Received 4 July 1995; revised version received 15 April 1996; accepted 3 May 1996)

## Abstract

*Chemical reaction between silicon nitride ceramic and iron metal was studied experimentally with diffusion couples at 1100–1150°C in order to clarify mechanisms in direct bonding of Si<sub>3</sub>N<sub>4</sub> to Fe-based alloys. The reaction products have been characterized and related to the thermodynamic data available. The extent of reaction is controlled by the nitrogen gas pressure build-up at the metal–ceramic interface and the rate by silicon diffusion into the metal. Under the experimental conditions, only an Fe(Si) solid solution was formed with maximum silicon content of about 12 at%. No silicides were found at the metal–ceramic interface. Nitrogen gas evolved at the interface is removed by permeation through the metal and/or through pores. Annealing atmosphere and sintering aid materials in the ceramic may play a role in the interaction. © 1996 Elsevier Science Limited.*

## 1 Introduction

Silicon nitride ceramic is an attractive material for high-temperature applications because of its low weight, unique toughness, strength, good thermal shock and wear resistance, and good high-temperature properties such as resistance to creep and to corrosion by the utilization atmosphere. Because it is uneconomical to manufacture complex parts from the ceramic and because the properties of both metal and ceramic are needed, in many applications metal/ceramic joining is essential, the metal being in this case a high-temperature, high-alloy material often based on Ni and/or Fe. Direct, i.e. diffusion, bonding is one solution whereby the difficult high-temperature requirements can be met.

In diffusion bonding chemical reaction takes place between the metal and the ceramic, and the properties of the reaction product layer dictate the usefulness of the bond and thus of the whole assembly at high temperatures. The reaction product layer should provide a strong bond between the two dissimilar materials, which means:

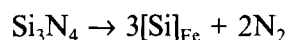
- (1) It should accommodate for the thermomechanical mismatch resulting from differences in thermal expansion coefficients (CTEs) of, in this case, Si<sub>3</sub>N<sub>4</sub> ( $3 \times 10^{-6} \text{ K}^{-1}$ ) and Fe ( $14 \times 10^{-6} \text{ K}^{-1}$ ) or Ni ( $15 \times 10^{-6} \text{ K}^{-1}$ ).
- (2) The reaction product layer should not consist of compounds that have mechanical properties significantly inferior to those of the metal and the ceramic. Silicides are brittle, they also have a different crystal structure (both Fe<sub>2</sub>Si and Fe<sub>3</sub>Si<sub>2</sub> are *hcp*) from the Fe-metal which is *fcc* for the low-Si  $\gamma$ -phase<sup>1</sup> (stable at 912–1394°C) and *bcc* for the  $\alpha$ -phase.

Thus it is evident that in our case silicide formation should be avoided, and that the first reaction product, Fe(Si) solid solution, should adhere strongly to the Si<sub>3</sub>N<sub>4</sub> ceramic and must not break at the  $\gamma/\alpha$ -boundary. The thickness of the reaction product layer can be controlled through the bonding time and temperature. As Fe-nitride formation is highly unlikely here,<sup>2</sup> the first reaction product is the binary Fe(Si) solid solution, with a very low solubility of nitrogen,<sup>3</sup> and the relative thicknesses of the parallel  $\gamma$ - and  $\alpha$ -phase layers depend on the respective interdiffusion coefficients.

When Si<sub>3</sub>N<sub>4</sub> reacts with non-nitride forming metal, the evolved N<sub>2</sub> gas must be removed from the metal–ceramic interface through cracks in the ceramic or along the interface, if possible, or by permeation through the metal or by a combination of these mechanisms. It may also be trapped, under high pressure, in pores in the interaction

\*To whom correspondence should be addressed.

zone but this can only be a small fraction of the total  $N_2$  production in view of the extreme pressures which would result. The pressure build-up can control the extent of the reaction through the dissociation constant of silicon nitride:



which gives

$$a_{Si}^3 \cdot p_{N_2}^2 = \text{constant} \quad (1)$$

Of previous studies, Weitzer and Schuster<sup>4</sup> annealed pure Fe and Fe–Si alloy/ $Si_3N_4$  powder mixtures, pressed into pellets, in evacuated quartz ampoules lined with Mo or Ta foil between 900 and 1150°C. At 900°C  $Si_3N_4$  coexists with all stable binary silicides and  $\alpha$ -Fe. At 1150°C  $Si_3N_4$  is decomposed by pure Fe, forming  $\alpha$ -Fe which contains 6–8 at% Si in solid solution. The partial pressure of  $N_2$  in the reactions was not specified.

Suganuma *et al.*<sup>5</sup> studied direct bonding of  $Si_3N_4$  to Fe at 1200 and 1400°C with diffusion couples using 30 min bonding times and external pressures of 100 and 10 MPa. The samples were hot-isostatically press(HIP)ed in glass capsules. The lower temperature is the same as that for the lower eutectic between the  $\alpha_1$ -solid solution and  $Fe_2Si$  ( $\beta$ ), so liquid phase formation was possible. At 100 MPa of external pressure a 20  $\mu m$  reaction layer with almost uniform Si content was formed on the metal side of the metal–ceramic interface, probably an  $\alpha$ -Fe(Si) solid solution (exact amount of silicon was not analysed). The authors also detected a thin  $Fe_5Si_3$  ( $\eta$ ) layer at the interface with  $Si_3N_4$  between the enrichment layer and the solid solution. However, according to the binary Fe–Si phase diagram,<sup>1</sup> the  $\eta$ -phase is only stable between 825 and 1060°C. Schiepers<sup>6</sup> annealed Fe/ $Si_3N_4$  diffusion couples at 1250°C under vacuum with the formation of a 500  $\mu m$  thick reaction zone which was a solid solution with a maximum of 7.3 at%  $[Si]_{Fe}$ . Peteves and Suganuma<sup>7</sup> used 200  $\mu m$  Fe and Fe–Cr foils as interlayers to join sintered  $Si_3N_4$  ceramics. Diffusion bonding was performed between 1100 and 1300°C for 1 h in Ar. They obtained sound bonds in all cases, under a uniaxial pressure of 50 MPa. The maximum solubility  $[Si]_{Me}$  and silicon penetration depth found at these temperatures was 1.5 at% and 25  $\mu m$ , respectively.

Engelvaart<sup>8</sup> studied the interaction of Fe and Fe–Cr alloys with  $Si_3N_4$  at 1100, 1150 and 1300°C under vacuum or  $10^5$  Pa of Ar or  $N_2$ . Using pure Fe he found the solid solution, but no silicides, as the reaction product. In Fe–Cr alloys, however, precipitates of chromium nitrides were also formed in the solid solution. With nitridation experiments nitrogen was found to permeate readily through Fe(Si) and Fe(Cr,Si) solid solution.

In this paper we shall take a closer look at some of the phenomena involved, using diffusion couple experiments.

## 2 Materials and Methods

The dense HPSN (hot-pressed silicon nitride) for the 5 by 5 mm diffusion couples was manufactured by ESK (Germany). It contains MgO and  $Al_2O_3$  (in total 1.5 wt%) as sintering aids. The Fe foil was supplied by Goodfellow Metals (UK). It is >99.99% pure Fe; impurities (in ppm): Ca = 1, Cr <1, Cu = 1, Mg <1, Si <1, C <50, H <1, N = 260 and O = 30. The metal surface to be joined was polished down to 1  $\mu m$  finish and the ceramic surface to 3  $\mu m$ . The Ar + 10 vol%  $H_2$  gas mixture was supplied by Oy Aga Ab (Finland) with  $N_2$  <10 ppm.

The diffusion couples were of sandwich type  $Si_3N_4/Fe/Si_3N_4$ . The experiments took place mainly in a horizontal mullite tube furnace with a helical SiC heating element. The couples were fixed in a ceramic spring clamp jig to allow uniaxial pressure to be applied to the sample. The heating rate was 300°C h<sup>-1</sup> and cooling took place within the furnace, after switching the power off, at about the following rates: over the temperature range 1100–800°C at approximately 250°C h<sup>-1</sup>, from 800 to 400°C at about 70°C h<sup>-1</sup> and thereafter at 15°C h<sup>-1</sup> to room temperature. A number of couples were annealed in a vacuum furnace ( $10^{-5}$  Pa), under uniaxial load of 5 MPa, with heating and cooling rates of 300 and 600°C h<sup>-1</sup>, respectively. After experiments the samples were mounted in plastic, sawn into two parts, polished, and studied by optical microscopy, scanning electron microscopy (SEM) and electron probe microanalysis (EPMA).

## 3 Results and Discussion

The interaction reaction can be characterized by studying the evolved microstructure, diffusion and the reaction restraints set by thermodynamics.

### 3.1 Microstructure

In Fig. 1 the morphology of the reaction zone in the Fe/ $Si_3N_4$  diffusion couple after annealing at 1100°C under Ar + 10 vol%  $H_2$  gas mixture (with total pressure  $10^5$  Pa) for 15 h is shown. The transition zone between the metal and the ceramic is characterized by precipitates of sintering aid materials and pores (see also Fig. 2). The Kirkendall plane (K), marked in the picture, indicates the position of the original  $Si_3N_4$  ceramic (marked by

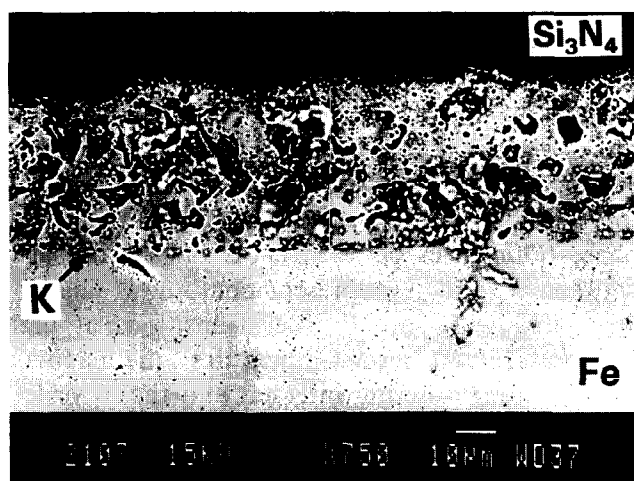


Fig. 1. Secondary electron image of the cross-section of an Fe/ $\text{Si}_3\text{N}_4$  diffusion couple annealed for 15 h at  $1100^\circ\text{C}$  under Ar + 10 vol%  $\text{H}_2$  gas mixture (with total pressure  $10^5$  Pa). K indicates the position of the Kirkendall plane.

sintering additives) that has been converted into an Fe(Si) solid solution. The maximal Si content of metal in the interaction zone is about 12 at% and the interaction zone thickness  $\approx 42 \mu\text{m}$ .

Figure 2 shows X-ray element maps of the diffusion couple interface region. Sintering aid elements Mg and Al are enriched together with Si in precipitates in the interaction zone where the ceramic has reacted and the metal phase (Fe) has moved towards it. Similar enrichment was also observed by Suganuma *et al.*<sup>5</sup> and Schiepers.<sup>6</sup> In some cases the couple was cracked on the ceramic side, approx-

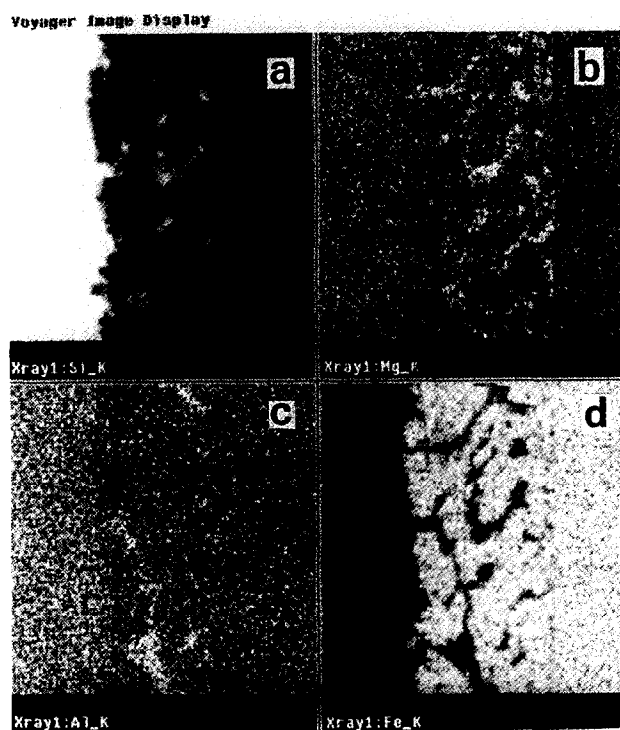


Fig. 2. X-ray element maps; (a)  $K_\alpha$  Si, (b)  $K_\alpha$  Mg, (c)  $K_\alpha$  Al and (d)  $K_\alpha$  Fe, of the interface region in an Fe/ $\text{Si}_3\text{N}_4$  diffusion couple. For experimental data, see Fig. 1.

imately parallel to the interface, and some tens of  $\mu\text{m}$  away from it, in a manner similar to that observed by Suganuma *et al.*<sup>5</sup> This shows that there is a good metal/ceramic bond but the ceramic was unable to accommodate the shrinkage of the metal on cooling.

### 3.2 Diffusion

An example of Si penetration curves measured in Fe/ $\text{Si}_3\text{N}_4$  diffusion couples is shown in Fig. 3 for two annealing times, 15 and 30 h, at  $1100^\circ\text{C}$  under Ar + 10 vol%  $\text{H}_2$  gas mixture. Silicon penetrates to a distance of  $>500 \mu\text{m}$  from the interface after 30 h of annealing. This indicates that the oxide/oxy-nitride layer or sintering aid enrichment layer, if any, at the metal–ceramic interface cannot act as a significant kinetic hindrance to prevent Si diffusion into the metal. Both penetration curves show a sharp drop at a silicon content in metal which is close to that for the  $\alpha/\gamma$  boundary, indicating that the diffusion rate in the  $\alpha$ -phase is higher than in the  $\gamma$ -phase. In both experiments the maximum concentration of silicon found in the metal near the metal–ceramic interface was about 12 at%. The increased scatter in the measured values near the interface is due to the presence of sintering aid precipitates which also contain Si.

The silicon penetration curves were subjected to Matano–Boltzmann analysis for graphical determination of interdiffusion coefficients. The values for the couples mentioned above are given in Fig. 4 along with values measured by Kodentsov *et al.*<sup>9</sup> for the Fe–Si system. The interdiffusion coefficients determined for Si concentrations of 10 and 7.5 at% ( $\alpha$ -phase) from the penetration curves in Fe/ $\text{Si}_3\text{N}_4$  diffusion couples are in good agreement with those reported for the binary Fe(Si) solid solution. This shows that iron–silicon interdiffusion in the metal is the rate-determining step, obviously

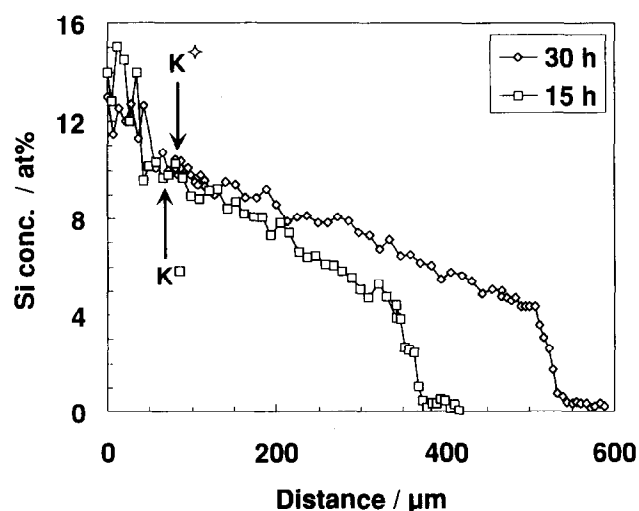


Fig. 3. Concentration profiles of silicon across the metal phase of Fe/ $\text{Si}_3\text{N}_4$  diffusion couples annealed for 15 ( $\square$ ) and 30 ( $\diamond$ ) h at  $1100^\circ\text{C}$ . K denotes the Kirkendall planes for both couples.

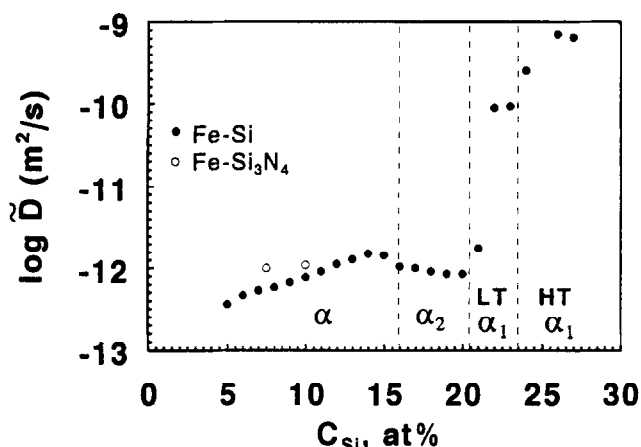


Fig. 4. Interdiffusion coefficients at 1100°C determined by Matano-Boltzmann analysis in Fe/Si diffusion couples at 5–27 at% Si<sup>9</sup> (●) and in Fe/Si<sub>3</sub>N<sub>4</sub> diffusion couples at 7.5 and 10 at% Si (○). The symbols  $\alpha$ ,  $\alpha_2$  and  $\alpha_1$  refer to the corresponding regions in the Fe(Si) solid solution, Fig. 5. LT and HT indicate low- and high-temperature modification of the ordered  $\alpha_1$  solid solution (DO<sub>3</sub>), respectively.

hardly influenced by the presence of nitrogen. In the  $\gamma$ -phase the interdiffusion is slower by about one order of magnitude. The Matano plane nearly corresponds to the position of the Kirkendall plane, indicating that at this temperature and composition Si and Fe have nearly equal mobilities.

In order to further elucidate the interaction mechanism, we will first take a closer look at the possible outcomes of the reaction as dictated by thermodynamics of the system Fe–Si–N.

### 3.3 Thermodynamics of the Fe–Si–N system

The Fe–Si binary phase diagram according to Kubaschewski<sup>1</sup> is reproduced in Fig. 5. The region of Fe(Si) solid solution contains two main phases:  $\gamma$ -phase (crystal structure *fcc*) and  $\alpha$ -phase (*bcc*). The body-centred cubic phase exists in disordered ( $\alpha$ -Fe) and ordered ( $\alpha_2$  and  $\alpha_1$ ) modifications. The phase boundaries between  $\alpha$ -Fe and  $\alpha_2$  and also between  $\alpha_2$  and  $\alpha_1$  represent continuous changes associated with second-order transitions at high temperatures. At lower temperatures, the magnetic and chemical ordering interact, and the  $\alpha_1$  ordering becomes a first-order reaction.<sup>10</sup>

The stable phases in the temperature range 1100–1150°C, in which the experiments were done, are  $\gamma$ -phase,  $\alpha$ -phase, Fe<sub>2</sub>Si, FeSi and Fe<sub>3</sub>Si<sub>7</sub> ( $\zeta_\alpha$ -FeSi<sub>2</sub>(HT), a high temperature phase). The  $\alpha$ - $\gamma$  boundary at 1100°C is at about 1.7 wt% Si (3.3 at%). The dissolution of nitrogen in the Fe(Si) solid solution ( $\gamma$  in equilibrium with 10<sup>5</sup> Pa N<sub>2</sub> gas) is negligible<sup>3</sup> at about 10<sup>-3</sup> at% at 1100°C. Except for Si<sub>3</sub>N<sub>4</sub>, no other solid Si–N compounds are known to exist.<sup>11</sup>

The thermodynamic data available for the Fe–Si binary<sup>12</sup> are shown in Fig. 6, from which we can see that the most stable silicide is FeSi. However, the scatter in the known Gibbs energy of formation ( $\Delta_f G^\circ$ ) values here is about  $\pm 5$  kJ at<sup>-1</sup>. Some data exist for the Fe(Si) solid solution, but they are mainly for dilute alloys,  $X_{\text{Si}} < 0.1$ . The data for the solid solution given here are

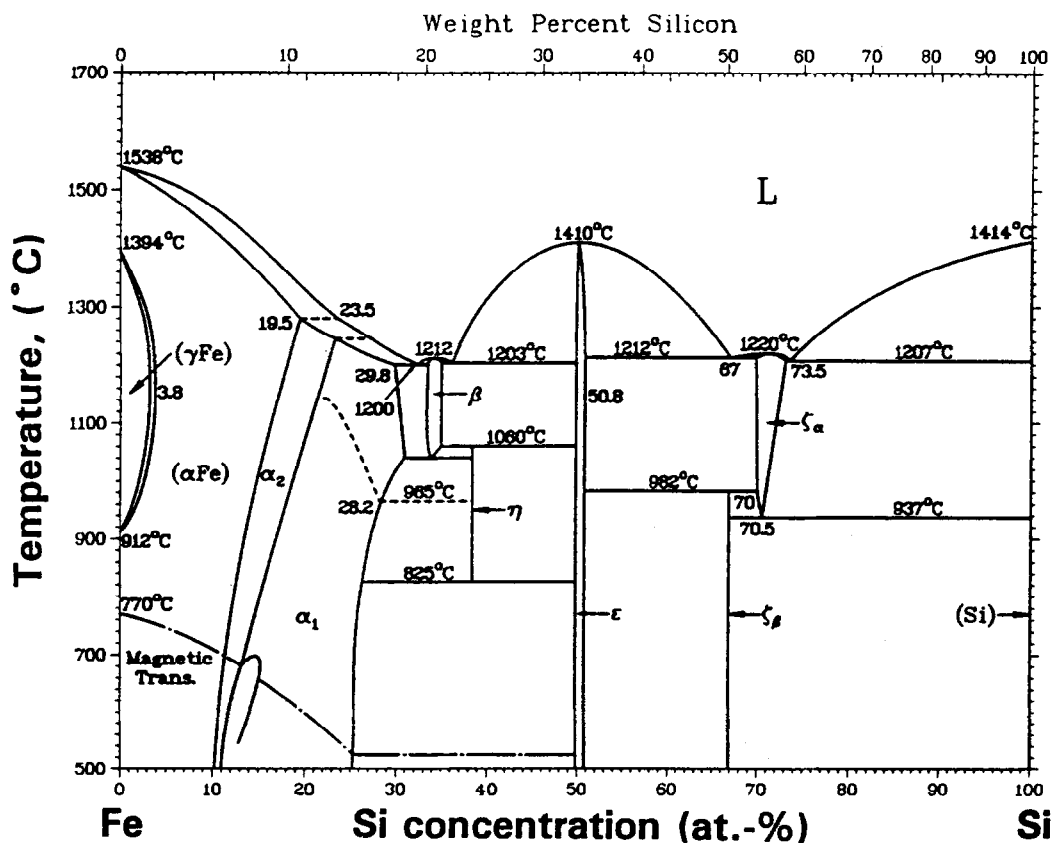


Fig. 5. The Fe–Si phase diagram.<sup>1</sup>

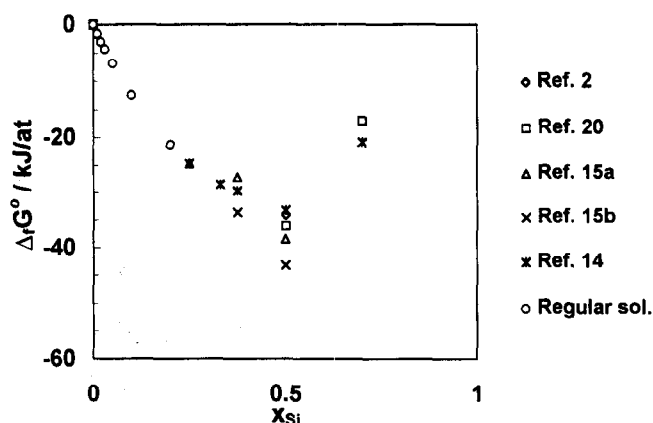


Fig. 6. Standard Gibbs energy of formation<sup>12</sup> for iron silicides at 1100°C.

calculated with the help of the  $\Omega$ -parameter,<sup>13</sup> assuming regular solution behaviour, and starting from the SGTE<sup>14</sup> databank value  $\Delta_f G^\circ$  for  $X_{\text{Si}} = 0.25$  of  $-24.73 \text{ kJ at}^{-1}$ . Ruzinov and Gulyanitskiy<sup>15</sup> quote two different  $\Delta_f G^\circ$  values for  $\text{FeSi}$  and  $\text{Fe}_5\text{Si}_3$ .

In Fig. 7 we present a  $p_{\text{N}_2} = f(T)$  stability diagram showing regions of the solid solution and the silicides in equilibrium with  $\text{Si}_3\text{N}_4$  as a function of nitrogen pressure. It was calculated using the Thermo-Calc program,<sup>16</sup> using data of Hillert *et al.*<sup>17</sup> for  $\text{Si}_3\text{N}_4$  and SGTE data, available in Thermo-Calc, for the Fe-Si system, assuming that ordering reactions and magnetic effects in the solid solution can be ignored. This may be a

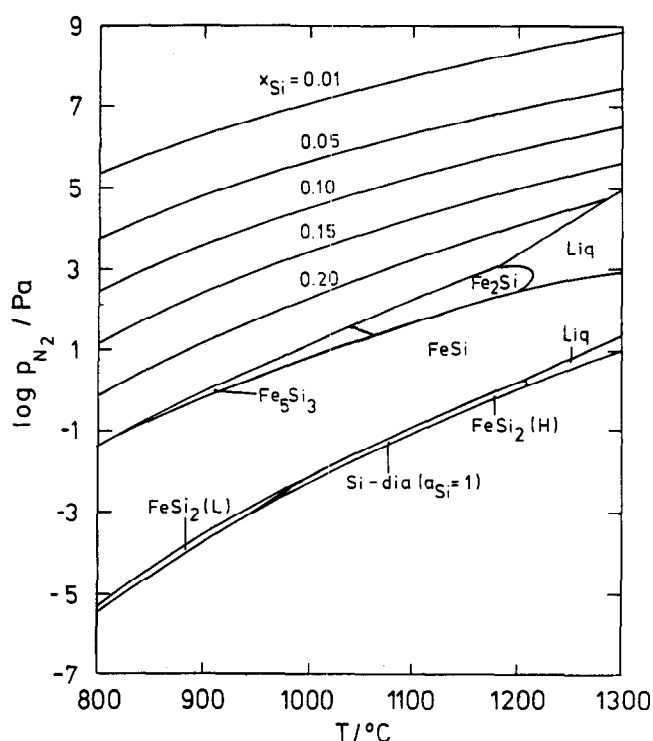


Fig. 7. Stability diagram for the Fe-Si-N system, calculated with the Thermo-Calc program, and showing the phases in equilibrium with  $\text{Si}_3\text{N}_4$  as a function of nitrogen partial pressure and temperature.

coarse simplification, but it should give us an estimate of the nitrogen pressure for each phase in equilibrium with  $\text{Si}_3\text{N}_4$ . At the  $\text{Fe}_2\text{Si}/\alpha$ -boundary at 1100°C the equilibrium  $p_{\text{N}_2}$  is about  $10^2 \text{ Pa}$  and  $p_{\text{N}_2} = 10^5 \text{ Pa}$  corresponds to an interface composition of  $[\text{Si}]_{\text{Fe}}$  of about 11–12 at%.

### 3.4 Nitrogen pressure build-up

Figure 8 shows the backscattered electron image of the cross-section of the diffusion couple annealed for 16 h under vacuum,  $\sim 10^{-5} \text{ Pa}$ , at 1150°C. The metal has deformed sufficiently at the outer edge to confirm the presence of a good contact between the diffusion couple halves. The width of the reaction zone, and (simultaneously) the Si content near the metal-ceramic interface, increase towards the edge. Close to the edge the concentration of silicon near the metal-ceramic interface is about 12 at% whereas in the central part of the couple it is only about 5 at%. This is a direct outcome from the mechanism of nitrogen removal from the reaction zone, which probably takes place mainly by permeation through the metal: the longer the distance to the outer surface and free atmosphere, which in this case was a dynamic vacuum, the more difficult it is for the nitrogen to escape. This results in a higher pressure at the interface and, correspondingly (see Fig. 7), in a lower Si content of the metal.

In the experiment shown in Fig. 8 the metal is clearly deformed, effectively sealing the interior of the couple from the outside atmosphere, and this leads to the kind of reaction mechanism described in the previous section. In the sample shown in Fig. 1 there was no such deformation at the edges, and the nitrogen gas evolved could also escape from the middle of the couple through the

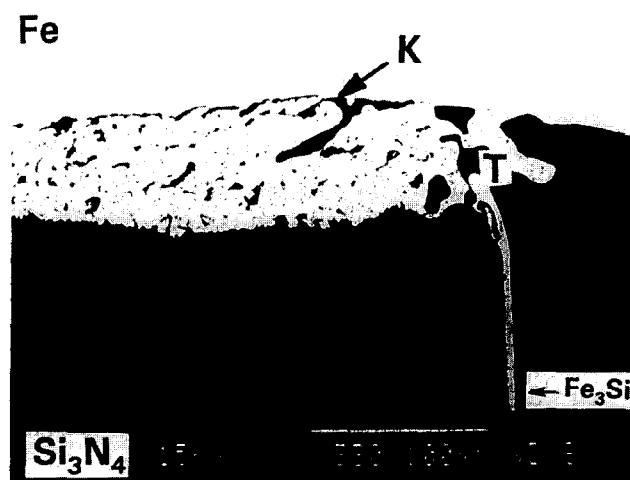


Fig. 8. Cross-section near the edge of an Fe/ $\text{Si}_3\text{N}_4$  diffusion couple annealed for 16 h at 1150°C under vacuum ( $10^{-5} \text{ Pa}$ ). T = triple point  $\text{Si}_3\text{N}_4$ -metal-gas; K = Kirkendall plane. (Backscattered electron image.)

interface or through open porosity. The silicon content in the metal and the width of the interaction zone were constant along the whole interface and the maximum silicon content found in this couple was the same (about 12 at%) as that near the edges of the deformed couple. In some couples the outside surface of the ceramic was covered by a metal-like layer which was analysed to be  $\text{Fe}_3\text{Si}$ . The metal had spread over the ceramic by surface diffusion, and  $\text{Fe}_3\text{Si}$  is the fastest of all Fe-silicides to grow, eating up the others if they are formed.<sup>9</sup>

In diffusion couples, the amount of silicon detected in the metal phase close to the metal–ceramic interface is 10–12 at%, and, referring to Fig. 7, we can deduce that  $p_{\text{N}_2}$  prevailing at the interface is  $\approx 10^5$  Pa. We cannot tell exactly the correspondence between the furnace atmosphere and that at the metal–ceramic interface, but as the couples were annealed at  $p_{\text{N}_2} \approx 1$  Pa (Ar + 10 vol%  $\text{H}_2$  mixture) or under vacuum, it is clear that nitrogen pressure is significantly increased at the interface by the interaction reaction. The low  $\text{N}_2$  pressure is responsible for the formation of an  $\text{Fe}_3\text{Si}$  layer at the edges of the couple where no pressure build-up takes place.

It is interesting to make a comparison between the phenomena observed here with iron and those with nickel, in interaction with  $\text{Si}_3\text{N}_4$  (Heikinheimo *et al.*<sup>18</sup>). Nickel silicides are more stable, i.e. the equilibrium nitrogen pressure at the solid solution/first silicide boundary with nickel at 1100°C is at a significantly higher pressure than with iron:  $10^6$ – $10^7$  versus  $10^2$  Pa. Also, in the case of nickel only a solid solution was found as the reaction product with maximum Si content of about 15 at%, and the pressure build-up was estimated as  $>3 \times 10^6$  or  $>9 \times 10^6$  Pa, depending on the  $\Delta_f G^\circ$  value selected for  $\text{Si}_3\text{N}_4$ . The microstructure near the Ni– $\text{Si}_3\text{N}_4$  interface is similar, with sintering aid precipitates and a well-defined Kirkendall plane. Silicon diffuses readily into the metal ( $\approx 300 \mu\text{m}$  at 1137°C, 30 h) and the interdiffusion process in the solid solution is the rate-determining step, as shown by Gülpen *et al.*<sup>19</sup> by Matano–Boltzmann analysis of penetration curves in Ni/ $\text{Si}_3\text{N}_4$  and Ni/ $\text{Ni}_3\text{Si}$  diffusion couples.

#### 4 Conclusions

When diffusion bonding pure iron to  $\text{Si}_3\text{N}_4$  ceramic at 1100–1150°C, chemical reaction takes place leading to the formation of an Fe(Si) solid solution phase where the maximum Si-content at the metal–ceramic interface corresponds to an equilibrium under increased nitrogen pressure. No Fe silicides were found at the metal–ceramic inter-

face. Silicon penetrates deep into the metal, up to about 500  $\mu\text{m}$  after 30 h of annealing at 1100°C. Matano–Boltzmann analysis showed that interdiffusion coefficients in the solid solution are in good agreement with those in the binary Fe–Si system, and that Fe–Si interdiffusion in the Fe(Si) solid solution is the rate-determining step. A significant part of the nitrogen resulting from the interfacial reaction cannot be dissolved in the solid solution or be trapped in pores, and is removed from the contact surface probably by permeation through the metal. The exact mechanism for this is a subject for further studies.

#### Acknowledgements

E. H. and I. I. thank Professor L. Holappa for useful discussions, for supporting this study and for giving them appropriate facilities at HUT. E. H. is deeply grateful to Dr J. Klomp, now retired, for initiation and guidance during his first steps towards this challenging subject. Mr R. Luoma, presently at Outokumpu Co., deserves credit for expert assistance in the use of the Thermo-Calc program.

#### References

1. Kubaschewski, O., *Iron Binary Phase Diagrams*. Springer, Berlin, 1982, pp. 136–138. The Fe–Si phase diagram shown here is taken from Massalski, T. B. (ed.), *Binary Alloy Phase Diagrams*, 1st edn. ASM, Metals Park, OH, 1986, Vol. 2, p. 1108.
2. Knacke, O., Kubaschewski, O. & Hesselmann, K. (eds), *Thermochemical Properties of Inorganic Substances I*, 2nd edn. Springer, Berlin, 1991, p. 710.
3. Frisk, K., A thermodynamic evaluation of the Cr–N, Fe–N, Mo–N and Cr–Mo–N systems. *CALPHAD*, **15** (1991) 79–106.
4. Weitzer, F. & Schuster, J., Phase diagrams of the ternary systems Mn, Fe, Co, Ni–Si–N. *J. Solid St. Chem.*, **70** (1987) 178–184.
5. Suganuma, K., Okamoto, T., Koizumi, M., Fujita, T. & Niihara, K., Joining of silicon nitride with metallic interlayers. In *High Technology Joining. BABS 5th International Conference*, Brighton, UK, 3–5 November 1987, pp. 10/1–10/8.
6. Schiepers, R., The interaction of SiC with Fe, Ni and their alloys. PhD Thesis, Technical University of Eindhoven, 1991.
7. Peteves, S. D. & Suganuma, K., Solid state bonding of  $\text{Si}_3\text{N}_4$  ceramics with Fe–Cr alloy interlayers, *Ceram. Trans.*, **35** (1993) 229–238.
8. Engelaart, M. J. P., High-temperature reactions of silicon nitride with Fe–Cr alloys. MSc Thesis, Delft University of Technology, October 1993.
9. Kodentsov, A. A., Gülpen, J. H. & van Loo, F. J. J., Diffusion bonding of non-oxide ceramics to transition metals: interfacial microchemistry. In *Proceedings of the Fourth Euro Ceramics Conference, Joinings and Coatings*, Riccione, Italy, eds B. S. Tranchina & A. Bellosi. Gruppo Editoriale Faenza Editrice S.p.A., Italy, 1995, Vol. 9, pp. 3–10.

10. Lacaze, J. & Sundman, B., An assessment of the Fe-C-Si system. *Met. Trans. A*, **22** (1991) 2211–2223.
11. Gurvich, L. V., Veyts, I. V. & Alcock, C. B. (eds), *Thermodynamic Properties of Individual Substances*, 4th edn. Hemisphere Publ. Co., NY, 1991, Vol. 2, Part 1, pp. 297–298.
12. Isomäki, I., Chemical interaction of silicon nitride ceramic with iron. MSc Thesis, Technical University of Helsinki, 1992.
13. Swalin, R. A., *Thermodynamics of Solids*, 2nd edn. J. Wiley and Sons, New York, 1972, pp. 141–148.
14. SGTE-database, Version H, Stockholm, Royal Inst. of Technology, 1990.
15. Ruzinov, L. P. & Gulyanitskiy, B. S., *Equilibrium Transformations of Metallurgical Reactions*. Izd. Metallurgiya, Moscow 1975, p. 134 (in Russian).
16. Sundman, B., Jansson, B. & Andersson, J.-O., ThermoCalc, a databank for calculation of phase equilibria and phase diagrams. *CALPHAD*, **9** (1985) 153–190.
17. Hillert, M., Jonsson, S. & Sundman, B., Thermodynamic calculation of the Si-N-O system. *Z. Metallkde*, **83** (1992) 648–654.
18. Heikinheimo, E., Kodentsov, A., van Beek, J. A., Klomp, J. T. & van Loo, F. J. J., Reactions in the systems Mo-Si<sub>3</sub>N<sub>4</sub> and Ni-Si<sub>3</sub>N<sub>4</sub>. *Acta Metall. Mater.*, **40** (1992), Suppl., S111–S119.
19. Gülpén, J. H., Kodentsov, A. A. & van Loo, F. J. J., Growth of silicides in Ni-Si and Ni-SiC bulk diffusion couples. *Z. Metallkde*, **86** (1995) 530–539.
20. Barin, I. *Thermochemical Data for Pure Substances I*. VCH, Weinheim, 1989, pp. 580–581.